

---

# TOWARD EFFICIENT SPEECH EMOTION RECOGNITION VIA SPECTRAL LEARNING AND ATTENTION

---

**HyeYoung Lee**  
 SPILab Corporation  
 Ulsan  
 uohesha@korea.ac.kr

**Muhammad Nadeem**  
 SPILab Corporation  
 Ulsan  
 mnadeem@spilab.kr

July 11, 2025

## ABSTRACT

Speech Emotion Recognition (SER) traditionally relies on auditory data analysis for emotion classification. Several studies have adopted different methods for SER. However, existing SER methods often struggle to capture subtle emotional variations and generalize across diverse datasets. In this article, we use Mel-Frequency Cepstral Coefficients (MFCCs) as spectral features to bridge the gap between computational emotion processing and human auditory perception. To further improve robustness and feature diversity, we propose a novel 1D-CNN-based SER framework that integrates data augmentation techniques. MFCC features extracted from the augmented data are processed using a 1D Convolutional Neural Network (CNN) architecture enhanced with channel and spatial attention mechanisms. These attention modules allow the model to highlight key emotional patterns, enhancing its ability to capture subtle variations in speech signals. The proposed method delivers cutting-edge performance, achieving the accuracy of 97.49% for SAVEE, 99.23% for RAVDESS, 89.31% for CREMA-D, 99.82% for TESS, 99.53% for EMO-DB, and 96.39% for EMOVO. Experimental results show new benchmarks in SER, demonstrating the effectiveness of our approach in recognizing emotional expressions with high precision. Our evaluation demonstrates that the integration of advanced Deep Learning (DL) methods substantially enhances generalization across diverse datasets, underscoring their potential to advance SER for real-world deployment in assistive technologies and human-computer interaction.

The code is publicly available at <https://github.com/spilabkorea/ser>.

## 1 Introduction

Speech constitutes a fundamental component of human interaction [1], serving as a primary medium through which individuals express and interpret emotions. As human-machine interaction systems continue to advance, enhancing communication between humans and machines has become increasingly critical [2]. One approach to achieve this is through the analysis of speech signals, which encapsulate a wealth of emotional and contextual information [3], enabling the representation of complex emotional responses to various objects, environments, and events [4]. SER is an automated technique for detecting emotions from speech signals. During the past two decades, significant research has focused on improving its precision and computational efficiency [5]. Recognizing human emotions is fundamentally complex yet crucial, serving as a benchmark for evaluating emotion recognition models. These models are trained to classify various emotional states, such as happiness, sadness, surprise, neutrality, boredom, disgust, anger, and fear [6] by extracting and analyzing spectral, prosodic, and voice quality features from speech data.

The SER pipeline consists of three fundamental stages: preprocessing, feature extraction, and classification [7]. During preprocessing, raw speech signals undergo filtering and transformation to enhance their suitability for analysis. Feature extraction subsequently derives salient descriptors from preprocessed signals—such as energy, pitch, prosodic features, and MFCCs—which have proven effective in capturing the spectral and temporal dynamics critical to emotion recognition in speech [8, 9].

Finally, the classification stage leverages Machine Learning (ML) or DL architectures to map the extracted feature representations to discrete emotional categories, enabling robust emotion recognition from speech signals [10]. The effectiveness of SER systems depends significantly on the accurate extraction and representation of spectral and temporal features, underscoring the importance of robust signal processing and feature engineering techniques.

Recently, research on emotion recognition has focused on improving feature extraction techniques to identify distinctive emotional patterns in speech signals. Early SER systems extensively relied on manually crafted features, including MFCCs, prosodic attributes (such as pitch, energy, and speaking rate), and spectral characteristics (like zero-crossing rate and formants) [8, 9]. Among these, MFCCs emerged as a benchmark standard due to their ability to approximate human auditory perception, effectively encoding spectral envelope information critical for emotion discrimination [11]. However, conventional methods frequently faced challenges in capturing temporal dynamics and contextual relationships, which restricted their effectiveness in intricate real-world situations. Advancements in transformer-based models have further enhanced the ability to capture nuanced emotional cues, addressing challenges such as valence gaps and improving generalizability across diverse datasets [12].

The advancement of DL algorithms has significantly enhanced the performance of SER. By leveraging DL-based approaches, researchers have effectively utilized features such as MFCC and Mel Energy-Spectrum Dynamic Coefficients (MEDC) to improve emotional state classification [13]. These methods reduce the dependence on manual feature engineering by enabling the automatic extraction of high-level, discriminative emotional patterns from speech signals. Convolutional Neural Networks (CNNs) have shown exceptional effectiveness in speech emotion recognition (SER) tasks, primarily because of their capability to extract hierarchical feature representations from speech data.

In this study, we propose a novel MFCC 1D-CNN model augmented with channel and spatial attention mechanisms to better recognize high-level emotional states in speech. The model’s performance is evaluated on 6 diverse benchmark speech emotion datasets: SAVEE [14], RAVDESS [15], CREMA-D [16], TESS [17], EMO-DB [18], and EMOVO [19].

This study addresses these challenges by introducing a framework that integrates MFCC feature extraction with data augmentation and attention-enhanced 1D-CNN. To increase the model’s robustness and generalizability, we integrate data augmentation methods, including noise injection and pitch modification, and techniques inspired by random cycle loss [20] to diversify the training dataset and strengthen its capacity to detect nuanced emotional cues.

The key contributions of this study are outlined as follows:

1. Our research focuses on developing a SER system using MFCC 1D-CNN. The proposed model leverages MFCC to extract features from audio data through a 1D-CNN network. This network effectively performed ablation analysis and demonstrated superior performance in speech emotion recognition.
2. A comprehensive analysis of the emotions expressed in the speech, the intricate aspects of language used, and the implicit signals in the SER. Existing research in SER often lacks a systematic emphasis on stable interaction modeling, limiting the ability to consistently detect emotional states and achieve optimal recognition precision. This work introduced MFCC 1D-CNN with channel and spatial attention. This model was designed to enhance feature extraction and facilitate the identification of the emotional class.
3. We evaluated the statistical and durability significance of our suggested model by analyzing 6 standardized datasets. SAVEE, RAVDESS, CREMA-D, TESS, EMO-DB, EMOVO. The model achieved accuracy rates of 97.49%, 99.23%, 89.31%, 99.82%, 99.53%, 96.39% for each dataset.

## 2 Related Work

SER represents a highly active area of research in affective computing. Manual extraction of acoustic features remains a dominant approach in current modeling research. During the 1990s, advancements in digital signal processing and ML led to the development of automated SER systems that utilized handcrafted acoustic features such as pitch, intensity, and spectral properties. Early research in SER frequently relied on traditional ML approaches, such as Support Vector Machines (SVMs), Gaussian Mixture Models (GMMs), and Hidden Markov Models (HMMs). However, with the emergence of DL in the 2010s, more sophisticated architectures such as Recurrent Neural Networks (RNNs), CNNs, and Transformer-based models revolutionized the field, leading to significant improvements in recognition accuracy and robustness.

Emotion recognition from speech has emerged as a key focus in the field of signal processing. Recent efforts have focused on deriving speech characteristics to improve classification precision. These models play a crucial role in identifying emotional conditions. Over the past ten years, models for speech emotion recognition have shifted from traditional ML methods to more advanced DL frameworks.

Suthar et al. [8] applied MFCC and SVM [21] for identifying emotional states and extracting features from speech signals. The SVM classifier processes the extracted features to classify emotions. This system is built for recognizing emotions in speech in real time. While MFCC condenses the speech signal into a set of key coefficients, SVM provides a computationally efficient and accurate framework for classifying emotional states.

Sugan et al. [22] utilized several frequency-scale-based triangular filter bank cepstral coefficients, such as linear scale human factor scale (HF), ERB-scale TFBCC-(E), TFBCC-(L), and bark-scale (B), and mel-scale TFBCC-(M). The extracted TFBCC features were combined and classified using an SVM classifier. For the EMO-DB dataset, the combination of TFBCC features based on Mel, Bark, and ERB scales resulted in the highest recognition accuracy of 86.96%. In contrast, the SAVEE dataset achieved a peak accuracy of 77.08% using a TFBCC configuration that incorporated Mel, Human Factor, and ERB frequency scales.

In a study by Othman [23] presented an emotion recognition system using MFCC features extracted from bio-signals. The system employs a Multi-Layer Perceptron (MLP) as the classifier. Experimental results demonstrate that the MFCC-MLP approach achieves up to 90% accuracy in emotion detection in EEG signals.

Akinpelu et al. [24] utilized a vision transformer [25] to enhance the precision of speech emotion classification. The TESS and EMO-DB datasets were employed to experimentally validate the effectiveness of the proposed technique. Their findings revealed a notable increase in speech emotion recognition accuracy, highlighting the model's ability to generalize across different datasets. The approach achieved accuracies of 98%, 91%, and 93% on the TESS and EMO-DB datasets, respectively.

Cooney et al. [26] investigates the use of different feature sets for classifying imagined speech EEG recordings, focusing on three feature sets: linear, non-linear, and MFCC. The dataset includes recordings of imagined speech production for eleven different speech units. The study shows that MFCC features offer superior classification performance as compared to other features.

Flower et al. [27] employed the Ramanujan Fourier transform for feature extraction and applied a multiclass SVM classifier in their study. They achieved recognition accuracies of 82.98% for the RAVDESS database, 83.08% for the Berlin database, 83.75% for the SAVEE database, and 82.99% on the EMOVO dataset. Jiang et al. [28] suggested LSTM and CNN to the temporal relationships and spectral characteristics to enhance the identification of emotional content in speech. The EMO-DB achieved an emotion identification accuracy of 84.53%. Tuncer et al. [29] proposed a method for identifying emotions in speech. This approach involves obtaining the distinctive attributes of the shuffle box, choosing relevant features through continuous neighborhood component evaluation, and employing an SVM classifier to classify emotions into distinct groups. The accuracy of emotion classification for the SAVEE, EMOVO, RAVDESS, EMO-DB, and datasets is 84.79%, 79.08%, 87.73%, 90.09% respectively. Ancilin et al. [30] employed multi-class SVM classifiers to classify emotions by utilizing the MFMC. The classification accuracy is 81.50% for the Berlin database, 64.31% for the RAVDESS database, 75.63% for the SAVEE database, and 73.30% for the EMOVO database. Pandey [6] examined the utilization of conventional speech representations, including MFCC, mel, and magnitude, for emotion classification by employing CNN and LSTM. The accuracy of the CNN + BiLSTM by using MFCC on the EMO-DB dataset was 82.35%. Laghari et al. [31] minimized noise in the speech data using an Optimally Modified Log-spectral Amplitude estimator (OMLSA). Furthermore, they applied white noise, pitch, and time-stretching to balance the dataset. Their proposed method achieved 91% and 88% accuracy for Sindhi and Urdu datasets. Changjiang et al. [32] proposed DCNN BiGRU self-attention by combining spatial characteristics of convolutional neural networks. Their method achieved the accuracy of 89.53% and 91.74% in the EMO-DB and CASIA [33] databases. Fang et al. [34] proposed a feature fusion technique that utilizes LSTM and 1D-CNN to extract both temporal and spatial elements. Zhao et al. [4] utilized a 2D-CNN-LSTM network to extract a log-mel spectrogram and achieved 95.89% precision in identifying emotions using the Berlin dataset. Xie et al. [35] examined WPD-based [36] textural and acoustic features for classifying speech emotions. In addition to this, they utilized a dual-stage feature selection procedure to decrease the number of dimensions and minimize the time required for model training. RAVDESS, SAVEE, EMOVO, and EMO-DB datasets achieved classification accuracies of 86.97%, 88.79%, 89.24%, and 95.29%, respectively. Mustaqeem et al. [37] employed CNNs for SER. However, incorporating feature selection can reduce the accuracy of SER. Recent advancements in SER have been achieved through the use of Neural Network (NN) techniques, such as CNN classifiers, combined with MFCC spectrogram features. Shahin et al. [38] stated that MFCC is a widely recognized technique for extracting features. The DC-LSTM outperforms traditional classifiers. The research findings indicate that when applied to the Arabic speech dataset using Emirati accent, the proposed method achieves an average accuracy of 89.3% in identifying emotions. Povilas et al. [39] utilized CNNs to extract features from acoustic systems, replacing traditional feature extraction methods with unsupervised approaches.

## 2.1 Multi Feature Based Emotion Recognition

Recognition of emotions using multiple features has attracted considerable interest because of its ability to enhance the precision and reliability of emotion classification systems. Traditional approaches typically focus on a single modality, such as speech, text, or facial expressions. However, recent studies have demonstrated that combining features from multiple modalities can offer complementary information, leading to enhanced performance. Various fusion strategies have been explored, including feature-level and decision-level fusion. For instance, audio features such as MFCC and filterbank energies, along with textual features derived from pre-trained language models like BERT [40] and RoBERTa [41] and visual cues such as facial expressions, have been successfully combined. Transformer-based architectures and attention mechanisms, particularly cross-modal attention, have been applied to model the interdependencies between these modalities, enabling better capture of complex emotional states. Transformer-based architectures and attention mechanisms, particularly cross-modal attention, have been applied to model the interdependencies between these modalities, enabling better capture of complex emotional states [42]. Furthermore, DL models such as CNNs, RNNs, and Gated Recurrent Units (GRUs) [43] have been employed to process and fuse multi-modal features. Recent work by Lian et al. [44] proposes a graph completion network to address incomplete multimodal learning in conversational settings, enhancing robustness in real-world scenarios. Incorporating depth information from databases like CAS(ME)3 [45] further improves the analysis of spontaneous micro-expressions, complementing speech-based features. Advancements in visual speech analysis [46] also highlight the synergy between acoustic and visual modalities for holistic emotion understanding. These approaches have shown promising results across several emotion recognition datasets, such as IEMOCAP [47], MELD [48], and others, addressing challenges related to modality alignment, feature redundancy, and dataset limitations. Moreover, learning emotion category representations across languages [49] enables systems to detect emotional relations in multilingual contexts, broadening the applicability of SER systems. Current research efforts are focused on developing improved methods for integrating multimodal features and enhancing the generalizability of emotion recognition models.

## 3 Datasets

The proposed study uses 6 distinct datasets (TESS, RAVDESS, CREMA-D, SAVEE, EMO-DB, EMOVO) to improve the ability to apply the acquired results in a broader range of situations. The detailed descriptions of the datasets are presented below.

1. The Ryerson Audio-Visual Database of Emotional Speech and Song (RAVDESS) [15]: RAVDESS is a widely adopted benchmark for speech emotion recognition (SER). It comprises 1,440 English utterances produced by 24 professional actors (12 male and 12 female), encompassing eight emotional categories: happiness, sadness, anger, fear, disgust, surprise, boredom, and neutrality.
2. TESS [50]: The TESS dataset contains 2,800 audio samples recorded by two female speakers articulating English sentences. These recordings represent eight distinct emotional expressions: anger, disgust, fear, happiness, sadness, surprise, boredom, and neutrality.
3. CREMA-D [16]: CREMA-D comprises 7,442 authentic audio clips produced by 43 female and 48 male performers representing diverse ethnicity including Hispanic, Asian, African, and American. There are 12 sentences that are used to represent six distinct emotions. The emotions included in this list include sadness, happiness, disgust, neutrality, rage, and fear.
4. Surrey Audio-Visual Expressed Emotion (SAVEE) [51]: The SAVEE dataset was developed using recordings from four male native English speakers—DC, JE, JK, and KL—who were postgraduate students at the University of Surrey, aged between 27 and 31. The dataset encompasses seven emotional classes: anger, disgust, fear, happiness, sadness, surprise, and neutrality, as commonly defined in psychological studies. Each speaker articulated 15 sentences per emotion, selected from the TIMIT corpus. This set included three sentences shared across all emotions, two that were emotion-specific, and ten general utterances tailored to each emotion, arranged in alphabetical order.
5. The EMO-DB [18]: The EMO-DB dataset, created by the Institute of Communication Science at the Technical University of Berlin, comprises emotional speech samples from ten professional actors—five male and five female. It contains 535 utterances covering seven emotional categories: anger, boredom, anxiety, happiness, sadness, disgust, and neutrality. The audio was initially recorded at a 48 kHz sampling rate and later resampled to 16 kHz for standardization.
6. The EMOVO [19]: The EMOVO dataset comprises Italian-language recordings collected from six actors, each delivering 14 sentences expressing six core emotional states—anger, disgust, fear, joy, sadness, and surprise—along with a neutral condition. These categories align with the commonly referenced 'Big Six'

emotions in speech emotion research. The recordings were produced using professional audio equipment at the laboratories of the Fondazione Ugo Bordoni.

## 4 Methodology

This section introduces our framework for SER. As presented in Fig. 4, our framework consists of MFCC features extraction, data augmentation, and a 1D CNN with channel and spatial attention.

### 4.1 Data Augmentation

To improve the robustness and variation in the dataset, we used two data augmentation techniques: noise and pitch. The noise addition process involves adding Gaussian noise to the audio data, achieved by generating random noise with an amplitude proportional to 3.5% of the maximum signal amplitude. The generated noise is added to the original audio, thereby simulating a more challenging and realistic audio environment. The pitch shifting technique, on the other hand, is implemented using the librosa library. The audio signal is shifted by four semitones, either upwards or downwards, effectively altering the pitch of the audio while preserving its other characteristics. These augmentation techniques substantially enlarge the dataset, helping the model perform better across diverse audio conditions.

$$x_{\text{noise}}(t) = x(t) + \alpha A_{\text{max}} \cdot \mathcal{N}(0, 1), \quad (1)$$

Where  $x(t)$ : original audio signal,  $A_{\text{max}}$ : maximum absolute amplitude of  $x(t)$ ,  $\alpha$ : noise scale factor (e.g., 0.035 for 3.5%),  $\mathcal{N}(0, 1)$ : standard normal distribution

$$x_{\text{pitch}}(t) = \text{PitchShift}(x(t), s), \quad (2)$$

Where  $x(t)$ : original audio signal,  $s$ : number of semitones to shift (e.g.,  $s = \pm 4$ ),  $x_{\text{pitch}}(t)$ : pitch-shifted audio signal

### 4.2 MFCC Feature Extraction

This article uses MFCC to extract characteristics from speech audio data. MFCC is a widely applied method for feature extraction in speech and audio analysis. It effectively captures the spectral characteristics of an audio signal by modeling human auditory perception. This technique is particularly valuable in applications such as speech recognition, speaker identification, and emotion recognition, as it highlights crucial frequency components of speech. The MFCC extraction process starts with pre-emphasis, which enhances higher frequencies, followed by segmenting the signal into overlapping frames using framing and windowing techniques. The Fast Fourier Transform (FFT) [52] is then applied to obtain the frequency spectrum. To simulate human auditory perception, the power spectrum is passed through a Mel filter bank, which employs a nonlinear frequency scale reflecting the ear's sensitivity to different frequency ranges. The resulting Mel-scaled spectrum undergoes a logarithmic transformation, and a Discrete Cosine Transform (DCT) [53] is applied to derive the final coefficients, which encapsulate the most relevant features of the signal. Compared to raw spectrograms, MFCC provides a more compact yet meaningful representation by eliminating redundant information and focusing on perceptually significant attributes. This makes it highly effective for ML and DL models for robust and discriminative features. Given these advantages, MFCC continues to be a fundamental component in various audio-based classification tasks, including automatic speech recognition, cochlear implant signal processing, and emotion analysis. MFCC features extraction includes various steps, which are discussed below. This section discusses not only the mathematical definitions of each process but also aspects of energy loss and feature preservation.

**Pre-Emphasis** To amplify the high-frequency components of the input signal  $x(t)$ , a pre-emphasis filter is applied. The resulting pre-emphasized signal, denoted as  $x'(t)$ , is computed using the following operation:

$$x'(t) = x(t) - \alpha \cdot x(t - 1), \quad (3)$$

where  $\alpha \in [0.9, 1.0]$  (commonly  $\alpha = 0.97$ ),

The pre-emphasis process is one of the main parts causing the energy loss of the signal, especially in the low frequency region. Let us briefly see why.

The formula for  $x'(t)$  can be rewritten as follows:

$$x'(t) = x(t) - \alpha \cdot x(t - 1) = (1 - \alpha)x(t) + \alpha\{x(t) - x(t - 1)\},$$

Let us explain why  $x'(t)$  is expected to be small in the case of low frequency. First, since  $\alpha$  is close to 1, the quantity  $(1 - \alpha)x(t)$  gets much smaller than  $x(t)$ . Moreover, if frequency is low, then  $x(t)$  oscillates slowly, so that the difference between adjacent values,  $x(t) - x(t - 1)$ , becomes smaller. This is why  $x'_n$  becomes much smaller when the frequency is low.

**Framing and Windowing** To prepare the signal for spectral analysis, it is divided into frames of length  $N$ , each overlapping with the previous by a hop size  $H$ . A window function  $w[n]$  is applied to every frame to reduce edge discontinuities. The windowed signal for each frame can be expressed as follows:

$$x_w[n] = w[n] \cdot x[n], \quad \text{for } n = 0, 1, \dots, N - 1 \quad (4)$$

where the window function  $w[n]$  is typically a Hamming window, defined as:

$$w[n] = a - (1 - a) \cdot \cos\left(\frac{2\pi n}{N - 1}\right), \quad \text{with } a = 0.54, \quad (5)$$

This step is where most of the energy loss is caused, which is mainly due to the framing window. This happens because the window function  $w[n]$  is less than or equal to 1, causing a significant reduction in energy, which is expressed as the sum of squared signal values, after windowing.

**Fast Fourier Transform (FFT)** Each frame  $x_w[n]$  is converted into the frequency domain through the application of the FFT:

$$X[k] = \sum_{n=0}^{N-1} x_w[n] \cdot e^{-j2\pi \frac{kn}{N}}, \quad k = 0, 1, \dots, N - 1, \quad (6)$$

Next, the magnitude spectrum is calculated as:

$$|X[k]|^2 = \text{Re}(X[k])^2 + \text{Im}(X[k])^2, \quad (7)$$

Mathematically, the energy of the original signal is the sum of the magnitude spectra, up to constant multiplication. This is due to the Plancherel's theorem:

$$\sum_{n=0}^{N-1} |x(n)|^2 = \frac{1}{N} \sum_{k=0}^{N-1} |X(k)|^2,$$

Therefore, there is no energy loss in the process of FFT.

**Mel Filter Bank Application** The Fourier spectrum is mapped to the Mel scale using a set of triangular Mel filter banks  $H_k(f)$ . Each Mel filter is defined as:

$$H_k(f) = \begin{cases} 0, & f < f_{k-1} \\ \frac{f - f_{k-1}}{f_k - f_{k-1}}, & f_{k-1} \leq f \leq f_k \\ \frac{f_{k+1} - f}{f_{k+1} - f_k}, & f_k \leq f \leq f_{k+1} \\ 0, & f > f_{k+1}, \end{cases} \quad (8)$$

where  $f_k$  is the center frequency of the  $k$ -th Mel filter. The Mel frequency is computed as:

$$m = 2595 \cdot \log_{10}\left(1 + \frac{f}{700}\right), \quad (9)$$

and the corresponding frequency  $f$  is:

$$f = 700 \cdot \left(10^{m/2595} - 1\right), \quad (10)$$

The Mel band energies  $M_k$  are computed by applying the Mel filter bank:

$$M_k = \sum_f |X[f]|^2 \cdot H_k(f), \quad k = 1, 2, \dots, K, \quad (11)$$

Since the sum of Mel filters is equal to 1, namely

$$\sum_k H_k(f) = 1$$

for all  $f$ , there is no loss of energy in this process.

**Logarithmic Transformation** The Mel band energies  $M_k$  are transformed to the logarithmic scale to mimic human auditory perception:

$$L_k = \log(M_k), \quad k = 1, 2, \dots, K, \quad (12)$$

This is merely a unit conversion to decibel (dB), so no energy is lost in this procedure. **Discrete Cosine Transform (DCT)** To convert the log-Mel spectrum to the cepstral domain, a DCT is applied. The DCT reduces correlation between Mel-frequency bands, leading to more compact and discriminative features:

$$\text{MFCC}_n = \sum_{k=1}^K L_k \cdot \cos \left[ n \cdot (k - 0.5) \cdot \frac{\pi}{K} \right], \quad n = 1, 2, \dots, N_{\text{coeff}}, \quad (13)$$

where  $N_{\text{coeff}}$  is the number of selected MFCC coefficients, typically the first 13 or 20 coefficients.

In general, DCT of  $N$  real values is equivalent to the FFT of  $4N$  values. In other words, the DCT of  $x(n)$ ,  $0 \leq n \leq N - 1$ , is equivalent to the FFT of  $y(n)$ ,  $0 \leq n \leq 4N - 1$ , where  $y(2n) = 0$  for  $0 \leq n \leq 2N - 1$ ,  $y(2n + 1) = x(n)$  for  $0 \leq n \leq N - 1$ , and  $y(4N - n) = y(n)$  for  $1 \leq n \leq 2N - 1$ . Hence, DCT does not consume energy for the same reason as FFT.

**Adaptive DCT as Eigen decomposition** The Discrete Cosine Transform (DCT) is reinterpreted as the eigendecomposition step. The DCT layer diagonalizes the feature covariance matrix. This approximates component decomposition by favoring bases that diagonalize the feature covariance matrix  $\Sigma_y$ , though full diagonalization is not explicitly enforced.

The DCT matrix is the orthogonal projection  $\mathbf{P} \in \mathbb{R}^{D \times F}$  that performs spectral decorrelation:

$$\mathbf{y} = \mathbf{P}^\top \mathbf{m}, \quad (14)$$

This adaptive DCT functions similarly to eigendecomposition by:

- **Diagonalizing the covariance matrix** of Mel energies (columns of the  $\mathbf{P}$  approximate principal components)
- **Ordering coefficients** by explained variance (through learned weight importance)
- **Allowing dimensionality reduction** through coefficient selection

### 4.3 MFCC in Preserving Spectral Features

In the previous subsection, we have seen that there is some energy loss when finding MFCCs of a signal. Nevertheless, the key spectral features are preserved during this process, which makes MFCC still significant.

To see this, let us give an example. Consider a sum of sinusoidal signals

$$\begin{aligned} x(t) &= f\left(\frac{t}{16000}\right), \quad 0 \leq t \leq 15999, \\ f(x) &= \frac{1}{M} (\sin 200\pi x + \sin 1000\pi x \\ &\quad + \sin 2000\pi x + \sin 4000\pi x), \\ M &= \max(\sin 200\pi x + \sin 1000\pi x \\ &\quad + \sin 2000\pi x + \sin 4000\pi x). \end{aligned}$$

In other words,  $x(t)$ 's are one-second-long samples with a sample rate of 16 kHz, of a sum of sinusoidal signals with frequencies (in Hz) 100, 500, 1000, and 2000, respectively. Hence, the key spectral features of  $x(t)$  are the frequencies 100, 500, 1000, and 2000. It is expected that the power spectra of  $x(t)$  are concentrated near those frequencies.

From Fig. 1 to 3, the power spectra of the signal  $x(t)$  are shown: that of the raw signal, pre-emphasized signal, and windowed signal, respectively.

The value  $x$  on the  $x$ -axis means the frequency  $31.25x$  (in Hertz), so one may see from the figures that the peaks of the spectra are located on the main frequencies of the raw signal. More precisely,  $x = 3.2, 16, 32$ , and  $64$  correspond to the frequencies 100, 500, 1000, and 2000, respectively.

In addition, the low-frequency components in Fig. 2 and 3 are noticeably weaker compared to those in Fig 1, which is expected due to the application of pre-emphasis. The spectral peaks in all three figures occur at the same locations; however, the lowest frequency component (around  $x = 3.2$ ) is less prominent in Fig. 2 and 3. Despite this, the relative order of spectral magnitudes is maintained. Specifically, in Fig. 2 and 3, the 2000 Hz component exhibits the highest power, followed by the 1000 Hz, 500 Hz, and 100 Hz components. This indicates that the MFCC representation effectively preserves the spectral characteristics of the original signal.

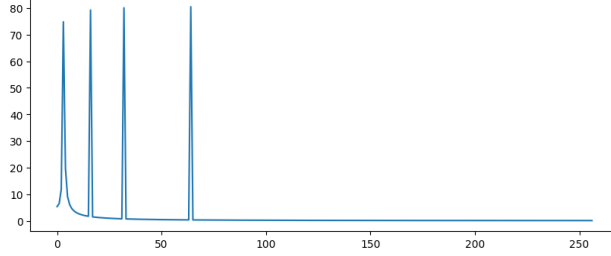


Figure 1: Spectrum of the raw signal  $x(t)$

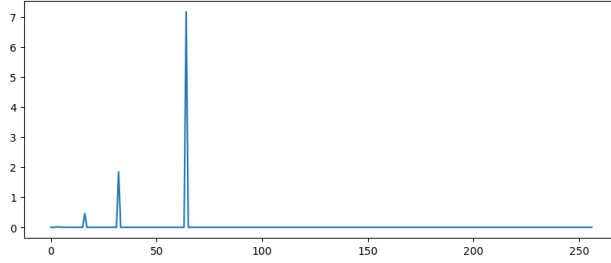


Figure 2: Spectrum of the pre-emphasized signal

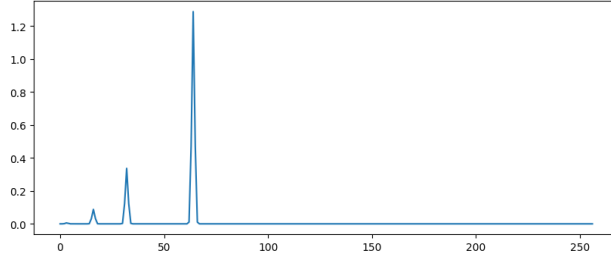


Figure 3: Spectrum of the windowed signal

#### 4.4 Cross-Entropy Loss for Multiclass Classification

To classify the extracted MFCC features for speech emotion recognition, we utilize the cross-entropy loss [54] function, a standard loss function for supervised classification tasks. The process involves applying the softmax function to the model's output to obtain the predicted class probabilities, which are then compared with the true label to calculate the loss.

**Cross-Entropy Loss** The cross-entropy loss is then computed using the predicted probabilities  $p_c$  from the softmax output and the true labels  $y_c$  (one-hot encoded). The cross-entropy loss is defined as:

$$\text{CE} = - \sum_{c=1}^C y_c \log(p_c), \quad (15)$$

where:



- $C$  is the total number of classes,
- $y_c \in \{0, 1\}$  indicates whether class  $c$  is the correct label,
- $p_c$  is the predicted probability for class  $c$ .

By applying the softmax function and computing the cross-entropy loss, the model is trained to minimize the error between the predicted probabilities and the true labels, which helps in the classification of speech emotion recognition.

**Probability Mapping via Softmax** For  $J$  anomaly classes, the final layer computes logits  $\mathbf{h} = [h_1, \dots, h_J]^T$  from  $\mathbf{z}$ :

$$\mathbf{h} = \mathbf{W}\mathbf{z} + \mathbf{b}, \quad (16)$$

where  $\mathbf{W} \in \mathbb{R}^{J \times k}$  and  $\mathbf{b} \in \mathbb{R}^J$  are learnable parameters. A softmax function converts these to class probabilities:

$$p_j = \frac{\exp(h_j)}{\sum_{i=1}^J \exp(h_i)}, \quad j = 1, \dots, J, \quad (17)$$

**Cross-Entropy as Separability Objective:** The cross-entropy loss  $\mathcal{L}$  measures divergence between predicted probabilities  $\mathbf{p}$  and true labels  $\mathbf{y}$ :

$$\mathcal{L}(\mathbf{y}, \mathbf{p}) = - \sum_{j=1}^J y_j \log p_j, \quad (18)$$

where  $y_j \in \{0, 1\}$  is the one-hot encoded ground truth.

#### 4.5 Model Structure

This research introduces a simple CNN model that utilizes MFCC features, enhanced by channel and spatial attention mechanisms. Fig. 4 illustrates the structure of the 1D-CNN model incorporating both channel and spatial attention mechanisms. The model comprises three convolutional blocks. Every convolutional block consists of a convolution operation, a batch normalization step, and a subsequent pooling layer. To handle the one-dimensional input vector, the convolutional layer performs a one-dimensional convolution. The sequence of the convolutional layers is presented in Table. 1. Batch normalization is used after each convolution layer to improve the efficiency of training and the performance of the neural network. Subsequently, Max pooling is then applied in each pooling layer to reduce the input data, selecting the highest value from a spatial window with a size of 7. The window is moved with a stride of 1. However, the output width remains the same as the input by using "same" padding. Following the convolutional blocks, we introduced the dense layer. The completely linked layer consists of 64 neurons, with the ReLU function acting as the activation function. Channel and Spatial attention module is integrated before the dense layer. The number of neurons in the final output layer is equal to the number of categories for speech emotions. The softmax function serves as the activation function.

**Channel and Spatial Attention** Attention mechanisms have been widely utilized in DL models to enhance feature representation by selectively focusing on important aspects of the input features. In this work, we incorporate both channel and spatial attention to improve the discriminative power of our speech emotion recognition model, which utilizes MFCC features as input and a 1D-CNN as the backbone architecture. Channel attention aims to emphasize informative feature maps while suppressing less relevant ones. In our model, we employ the Squeeze-and-Excitation (SE) mechanism to refine the extracted MFCC features. This mechanism consists of three key steps: squeeze, excitation, and scaling. The squeeze operation aggregates temporal information by applying global average pooling across each feature map. The excitation step utilizes fully connected layers followed by a sigmoid activation to generate per-channel attention weights. These weights are then used to scale the original feature maps, allowing the model to emphasize frequency components that are crucial for differentiating between emotions. By leveraging channel attention, the model can better capture variations in speech that contribute to emotional expression. Spatial attention complements channel attention by focusing on significant time-frequency regions within the MFCC feature maps. It captures temporal dependencies by computing an attention map that highlights key regions in the spectrogram-like MFCC representation. To achieve this, we apply a convolutional layer followed by a sigmoid activation, producing a spatial weighting matrix. This matrix is then used to modulate the input features, enabling the network to concentrate on emotion-relevant temporal segments in speech signals. By integrating spatial attention, the model becomes more sensitive to meaningful variations in speech patterns associated with different emotions. By incorporating both channel and spatial attention mechanisms, our approach enhances the ability of the 1D-CNN to extract and utilize essential emotional cues from MFCCs, leading to improved accuracy in speech emotion recognition. The architecture of channel and spatial attention is presented in Fig. 5.

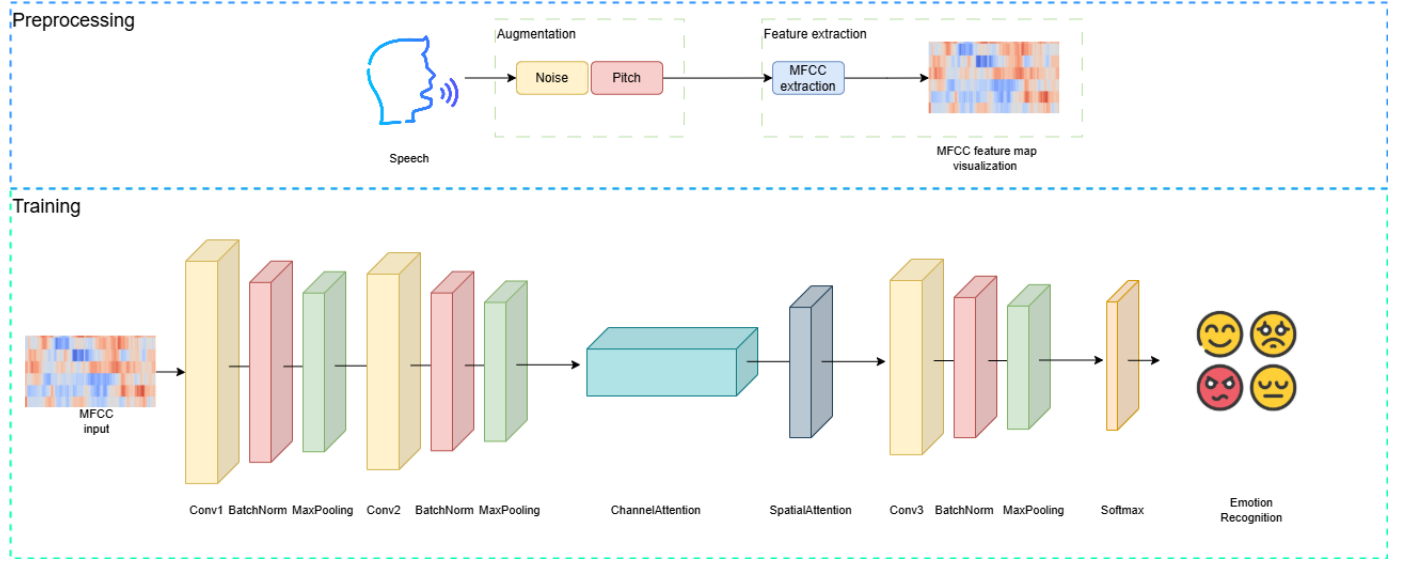


Figure 4: Main architecture of our proposed method

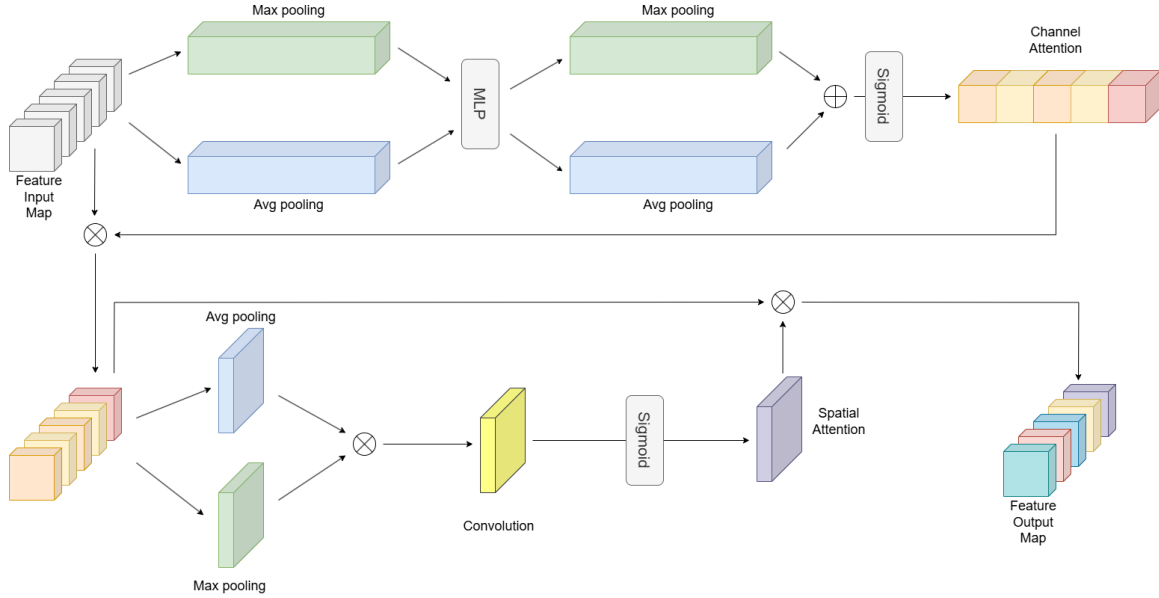


Figure 5: Channel and Spatial Attention Architecture

The mathematical representation for Spatial attention is as follows:

$$\mathbf{M}_s(F) = \sigma \left( f^{7 \times 7}([\text{AvgPool}(F); \text{MaxPool}(F)]) \right), \quad (19)$$

$$\mathbf{M}_s(F) = \sigma \left( f^{7 \times 7}([\mathbf{F}_{\text{avg}}^s; \mathbf{F}_{\text{max}}^s]) \right), \quad (20)$$

where  $\sigma$  denotes the sigmoid function and  $f^{7 \times 7}$  represents a convolution operation with a filter size of  $7 \times 7$ .

Similarly, for the Channel attention

$$\mathbf{M}_c(F) = \sigma \left( \text{MLP}(\text{AvgPool}(F)) + \text{MLP}(\text{MaxPool}(F)) \right), \quad (21)$$

$$\mathbf{M}_c(F) = \sigma \left( \mathbf{W}_1(\mathbf{W}_0(\mathbf{F}_{\text{avg}}^c)) + \mathbf{W}_1(\mathbf{W}_0(\mathbf{F}_{\text{max}}^c)) \right), \quad (22)$$

where  $\sigma$  denotes the sigmoid function,  $\mathbf{W}_0 \in \mathbb{R}^{C/r \times C}$ , and  $\mathbf{W}_1 \in \mathbb{R}^{C \times C/r}$ . Note that the MLP weights,  $\mathbf{W}_0$  and  $\mathbf{W}_1$ , are shared for both inputs, and the ReLU activation function is applied after  $\mathbf{W}_0$ .

Table 1: The parameter settings of our proposed method

Layer	Filters	Size of kernel	Strides	Padding	Activation function
1	256	7	1	same	relu
2	256	7	1	same	relu
3	Channel and Spatial Attention				
4	64	-	-	-	-

## 5 Experiments

### 5.1 Experimental Setting

For our experiment, we used the Adam optimizer [55] with an initial learning rate set to 0.00001. The dataset was split into training and testing using an 80:20 ratio. The batch size was configured to 64. To optimize the model, we minimized the cross-entropy loss function, performing a maximum of 100 iterations for parameter adjustment.

### 5.2 Evaluation metrics

Evaluating a model is crucial for improving its efficiency. Various metrics can be used to assess model performance. In this experiment, we used accuracy as the primary evaluation metric to measure and enhance the model's effectiveness. Accuracy is defined as the ratio of correctly predicted labels to the total number of observations. The classification accuracy is calculated using the following equation:

$$\text{Accuracy} = \left( \frac{TP + TN}{TP + TN + FP + FN} \right), \quad (23)$$

where the terms TP and TN stand for true positive and true negative, respectively. Similarly, FP and FN denote false positive and false negative.

### 5.3 Results

Table 2 presents a comparative analysis of classification accuracy between the proposed model and existing state-of-the-art methods for speech emotion recognition (SER), evaluated on six benchmark datasets: SAVEE [14], RAVDESS [15], CREMA-D [16], TESS [17], EMO-DB [18], and EMOVO [19].

Atial et al. utilized an attention-based 3CNN-LSTM model, achieving accuracies of 87.50% and 96.18% on the SAVEE and RAVDESS datasets, respectively. Ancilin et al. applied a modified MFCC feature set with an SVM classifier, resulting in accuracies of 75.63%, 64.31%, and 73.30% for SAVEE, RAVDESS, and EMOVO. Nagarajan et al. combined MFCC and Human-Factor Cepstral Coefficients (HFCC) with SVM, obtaining 77.03% on SAVEE and 86.96% on EMO-DB. Flower et al. introduced the Ramanujan Fourier Transform with SVM, achieving 83.75%, 82.99%, and 82.99% on SAVEE, RAVDESS, and EMOVO, respectively.

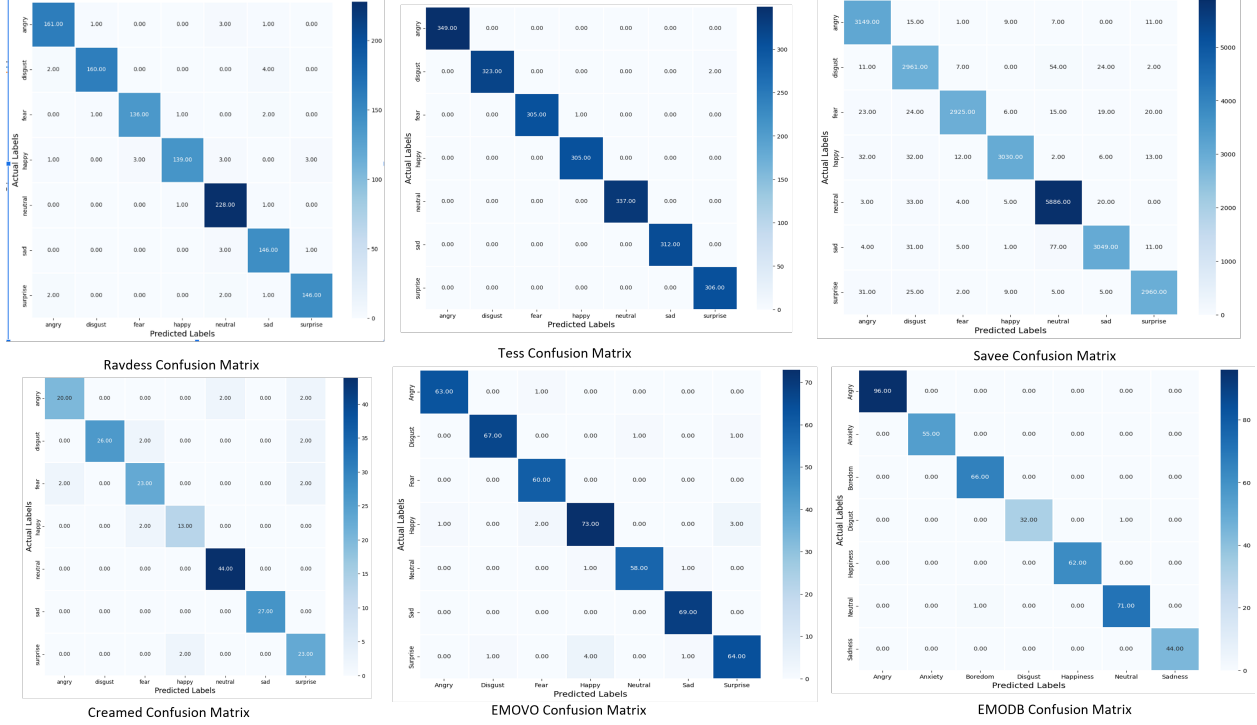


Figure 6: Confusion Matrices

Xie et al. employed Random Forest and Grey Wolf Optimization with early fusion, yielding 88.79%, 86.97%, 95.29%, and 89.24% on SAVEE, RAVDESS, EMO-DB, and EMOVO. Tuncer et al. used the Tunable Q Wavelet Transform with Iterative Neighborhood Component Analysis (INCA), achieving 84.79%, 87.73%, and 79.04% for SAVEE, RAVDESS, and EMOVO. Flower et al. also combined MFCC with Mel Frequency Magnitude Coefficients (MFMC) and utilized a 1D-CNN, reporting 91.70% and 98.10% on SAVEE and RAVDESS.

Sajjad et al. implemented a radial basis function network with BiLSTM, achieving 77.02% on RAVDESS and EMO-DB. Ristea et al. used a Self-paced Ensemble Learning method, yielding 68.12% on CREMA-D. Kilimci et al. bypassed feature extraction by directly feeding raw audio into a CNN, achieving 69.72% and 99.46% on CREMA-D and TESS. Mekruksavanich et al. used 1D-CNN with MFCC, reaching 65.77% on CREMA-D. Dharmyal et al. utilized prompt-based emotion descriptions, achieving 72.66% on CREMA-D. Gonçalves et al. employed versatile audiovisual learning, reporting 82.60% on CREMA-D. Krishnan et al. used a non-linear signal quantification method based on randomness measures, achieving 93.30% on TESS.

Meng et al. used BiLSTM with 3D Log-Mel Spectrograms, achieving 85.39% on EMO-DB. Liu et al. proposed a hybrid architecture combining two 1D convolutional layers, Transformer modules, and BiLSTM units, reaching 83.30% on SAVEE and 84.30% on EMO-DB. Dutt et al. combined 1D CNN-LSTM with wavelet transforms, achieving 81.40% on RAVDESS.

In contrast, our proposed model outperforms all existing methods, achieving state-of-the-art accuracy on all six benchmark datasets: 97.49% for SAVEE, 99.23% for RAVDESS, 89.31% for CREMA-D, 99.82% for TESS, 99.53% for EMO-DB, and 96.39% for EMOVO, as shown in Table 2.

Additionally, Fig. 7 provides a detailed visualization of the training and validation performance across six datasets. Specifically, Fig. 7(a) illustrates the training and validation accuracy and loss for the RAVDESS dataset, while Fig. 7(b) shows these metrics for the CREMA-D dataset. Similarly, Fig. 7(c) represents the training and validation accuracy and loss on the SAVEE dataset, Fig. 7(d) presents these metrics for the TESS dataset, Fig. 7(e) presents these metrics for the EMO-DB dataset, Fig. 7(f) presents these metrics for the EMOVO dataset.

Table 2: A comparative evaluation of the proposed method against State-of-the-Art (SOTA) techniques.

Study	SAVEE	RAVDESS	CREMA-D	TESS	EMO-DB	EMOVO
Atila et al.[10]	87.50	96.18	-	-	-	-
Ancilin et al. [30]	75.63	64.31	-	-	-	73.30
Nagarajan et al. [22]	77.03	-	-	-	86.96	-
Flower et al. [27]	83.75	82.99	-	-	-	82.99
Xie et al. [35]	88.79	86.97	-	-	95.29	89.24
Tuncer et al. [29]	84.79	87.73	-	-	-	79.04
Flower et al. [56]	91.70	98.10	-	-	-	-
Sajjad et al. [57]	-	77.02	-	-	77.02	-
Ristea et al. [58]	-	-	68.12	-	-	-
Kilimci et al. [59]	-	-	69.72	99.46	-	-
Mekruksavanich et al.[60]	-	-	65.77	-	-	-
Dhamyal et al. [61]	-	-	72.56	-	-	-
Goncalves et al. [62]	-	-	82.60	-	-	-
Krishnan et al. [63]	-	-	-	93.30	-	-
Meng et al. [64]	-	-	-	-	85.39	-
Liu et al. [65]	83.30	-	-	-	84.30	-
Dutt et al. [66]	-	81.40	-	-	-	-
<b>MFCC 1D-CNN + Channel Spatial Attention (Ours)</b>	<b>97.49</b>	<b>99.23</b>	<b>89.31</b>	<b>99.82</b>	<b>99.53</b>	<b>96.39</b>

#### 5.4 Ablation Study

To evaluate the contribution of MFCC features and data augmentation in SER using a 1D-CNN model, an ablation study was performed. Table 3 presents a comparative analysis of model accuracy across six benchmark SER datasets: TESS, RAVDESS, CREMA-D, SAVEE, EMO-DB, and EMOVO. The study considers four settings: (i) the baseline model without MFCC features and data augmentation, (ii) the model with MFCC features and data augmentation, (iii) the model using Chroma features, and (iv) the model using Chroma features without data augmentation.

The results show a substantial improvement in performance when MFCC features and data augmentation are applied. For instance, the accuracy on the TESS dataset increased from 84.01% to 99.82%, while RAVDESS improved markedly from 46.52% to 99.23%. Similar enhancements were observed for CREMA-D (41.82% to 89.31%) and SAVEE (46.35% to 97.49%). The EMO-DB and EMOVO datasets also showed notable gains, from 84.73% to 99.53% and from 84.70% to 96.39% respectively.

In comparison, models using Chroma features achieved relatively lower performance. For example, while TESS and EMOVO still performed well with accuracies of 98.30% and 93.41%, the RAVDESS and CREMA-D datasets achieved only 72.74% and 71.51%, respectively. SAVEE and EMO-DB reached 80.20% and 83.41% accuracy using Chroma features. When Chroma features were used without data augmentation, some datasets (e.g., SAVEE and EMO-DB) showed slight improvements—90.62% and 90.65% respectively indicating that augmentation has varying effects depending on the dataset.

Overall, these findings underscore the effectiveness of MFCC features combined with data augmentation in enhancing the generalization and robustness of SER models. While Chroma features offer moderate improvements over the baseline, they consistently underperform compared to MFCC-based representations. This highlights the superiority of MFCC features in capturing critical spectral characteristics relevant to emotion classification in speech.

Table 3: Accuracy of 1D-CNN model before applying MFCC features and augmentation, after applying MFCC and augmentation, with Chroma features, and Chroma without augmentation.

Dataset	Without MFCC and Augmentation (%)	With MFCC and Augmentation (%)	With Chroma Features (%)	With Chroma and without Augmentation (%)
TESS	84.01	99.82	98.30	98.92
RAVDESS	46.52	99.23	72.74	86.80
CREMA-D	41.82	89.31	71.51	86.31
SAVEE	46.35	97.49	80.20	90.62
EMO-DB	84.73	99.53	83.41	90.65
EMOVO	84.70	96.39	93.41	80.50

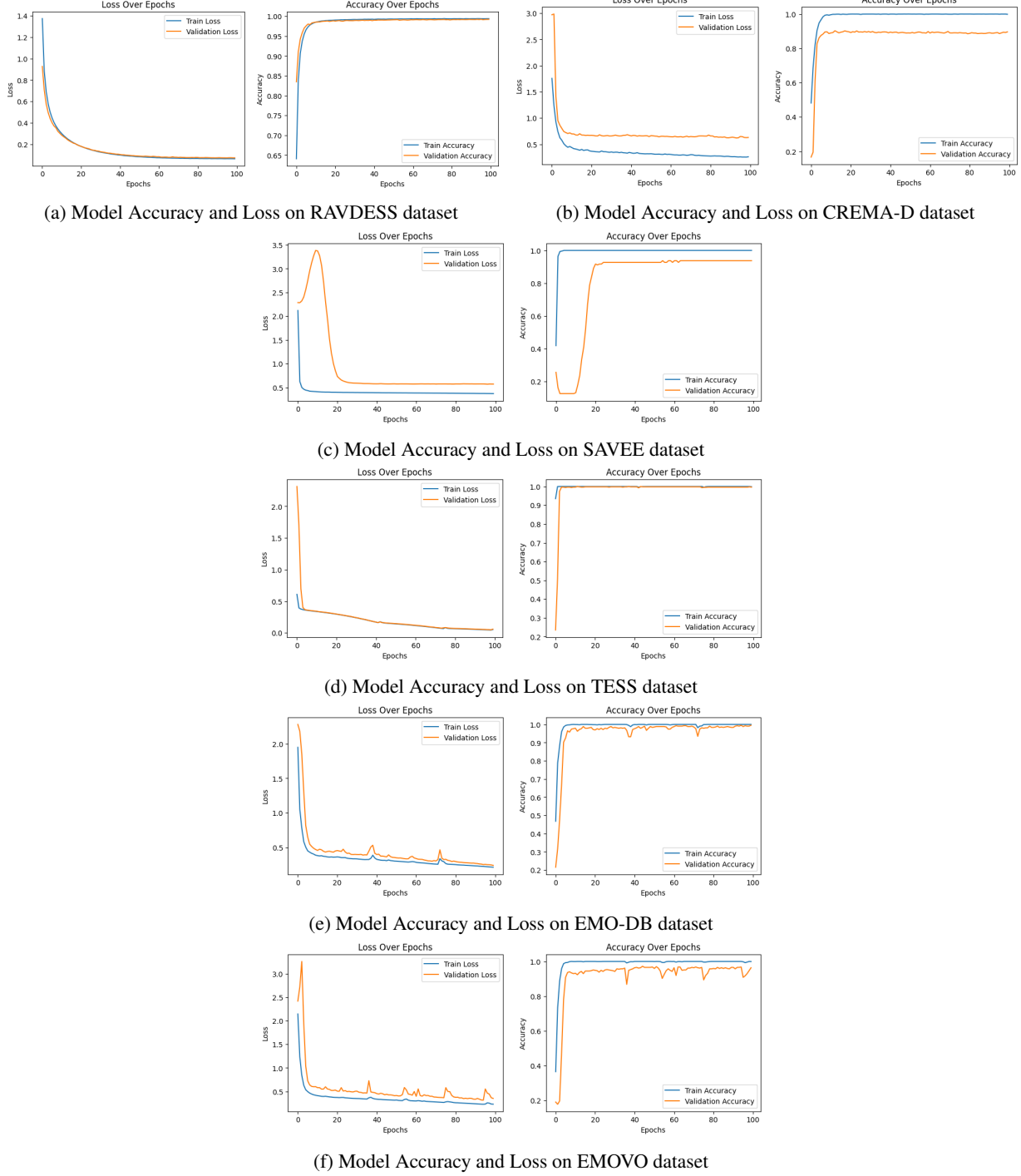


Figure 7: Training accuracy, loss, validation accuracy, loss graph of our proposed method on 6 datasets

## 6 Conclusion

This study introduced an MFCC 1D-CNN model enhanced with Channel and Spatial attention mechanisms for effective SER. The system involved preprocessing all audio samples by standardizing their duration and applying data augmentation techniques, such as adding noise and modifying pitch, to increase sample diversity. MFCC features were then extracted to capture the emotional states accurately, and these features were fed into the proposed 1D-CNN classifier. MFCC features are closely aligned with the way the human brain processes sound frequencies, making them

especially effective for recognizing emotional cues in speech across diverse datasets. We evaluated our system on 6 benchmark datasets: CREMA-D, RAVDESS, SAVEE, and TESS, EMO-DB, and EMOVO. The experimental results demonstrated high accuracy rates of 89.31% for CREMA-D, 94.75% for SAVEE, 99.82% for TESS, and 99.23% for RAVDESS, with 99.53% for EMO-DB and 96.39% for EMOVO. Our approach outperformed other state-of-the-art methods across these datasets, showcasing its effectiveness in emotion recognition. However, despite these promising results, the model showed relatively lower performance on the CREMA-D dataset, indicating room for improvement. To further enhance the model’s accuracy, future work will explore the integration of additional feature extraction techniques, such as combining spectral and prosodic features, which may provide more comprehensive emotional representation. Additionally, we plan to investigate further optimization of the attention mechanisms to improve the model’s generalization ability across diverse datasets. These future efforts aim to refine the model’s robustness, ensuring higher recognition performance and broader applicability in real-world SER applications.

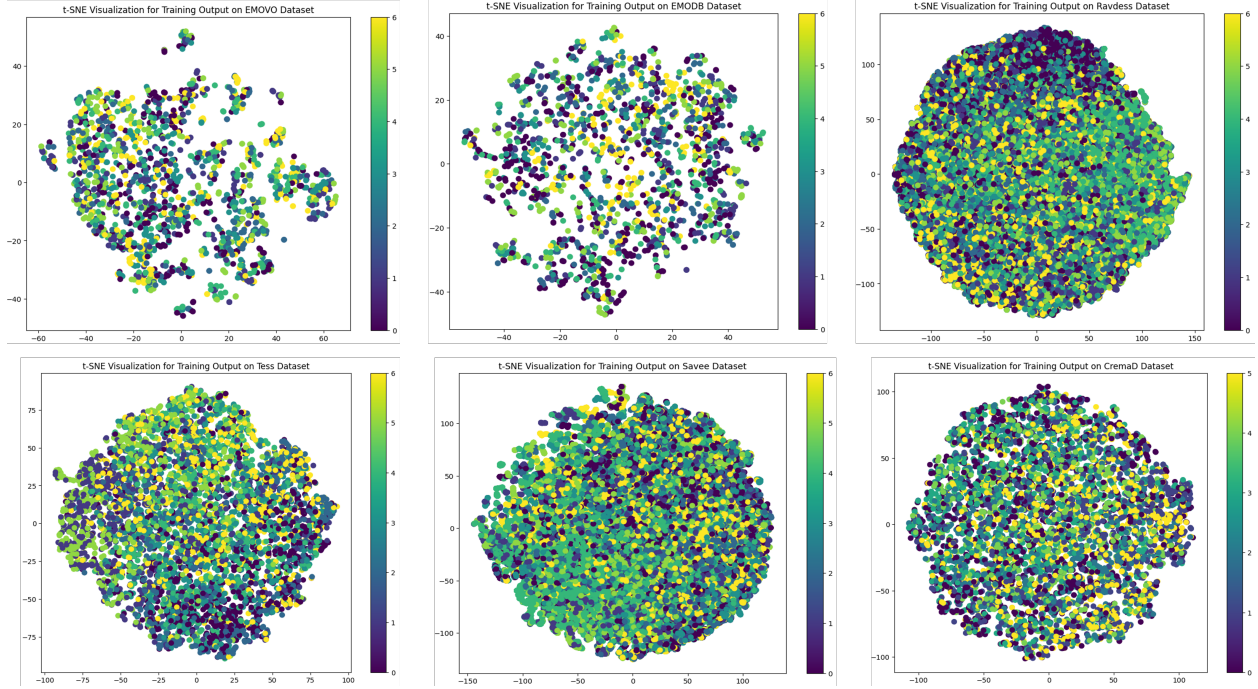


Figure 8: T-SNE Visualization

## References

- [1] Waleed Alsabhan. Human–computer interaction with a real-time speech emotion recognition with ensembling techniques 1d convolution neural network and attention. *Sensors*, 23(3):1386, 2023.
- [2] Roddy Cowie, Ellen Douglas-Cowie, Nicolas Tsapatsoulis, George Votsis, Stefanos Kollias, Winfried Fellenz, and John G Taylor. Emotion recognition in human-computer interaction. *IEEE Signal processing magazine*, 18(1):32–80, 2001.
- [3] Elham S Salama, Reda A El-Khoribi, Mahmoud E Shoman, and Mohamed A Wahby Shalaby. A 3d-convolutional neural network framework with ensemble learning techniques for multi-modal emotion recognition. *Egyptian Informatics Journal*, 22(2):167–176, 2021.
- [4] Jianfeng Zhao, Xia Mao, and Lijiang Chen. Speech emotion recognition using deep 1d & 2d cnn lstm networks. *Biomedical signal processing and control*, 47:312–323, 2019.
- [5] Monorama Swain, Bubai Maji, P Kabisatpathy, and Aurobinda Routray. A dcrnn-based ensemble classifier for speech emotion recognition in odia language. *Complex & Intelligent Systems*, 8(5):4237–4249, 2022.
- [6] Sandeep Kumar Pandey, Hanumant Singh Shekhawat, and SR Mahadeva Prasanna. Deep learning techniques for speech emotion recognition: A review. In *2019 29th international conference RADIOELEKTRONIKA (RADIOELEKTRONIKA)*, pages 1–6. IEEE, 2019.

- [7] Anusha Koduru, Hima Bindu Valiveti, and Anil Kumar Budati. Feature extraction algorithms to improve the speech emotion recognition rate. *International Journal of Speech Technology*, 23(1):45–55, 2020.
- [8] Ritu D Shah, Anil C Suthar, and ME Student. Speech emotion recognition based on svm using matlab. *International Journal of Innovative Research in Computer and Communication Engineering*, 4:2916–2921, 2016.
- [9] Shalbbya Ali, Safdar Tanweer, Syed Sibtain Khalid, and Naseem Rao. Mel frequency cepstral coefficient: a review. *ICIDSSD*, 2020.
- [10] Orhan Atila and Abdulkadir Şengür. Attention guided 3d cnn-lstm model for accurate speech based emotion recognition. *Applied Acoustics*, 182:108260, 2021.
- [11] Mihaela Costin and Marius Zbancioc. Improving cochlear implant performances by mfcc technique. In *Signals, Circuits and Systems, 2003. SCS 2003. International Symposium on*, volume 2, pages 449–452. IEEE, 2003.
- [12] Johannes Wagner, Andreas Triantafyllopoulos, Hagen Wierstorf, Maximilian Schmitt, Felix Burkhardt, Florian Eyben, and Björn W Schuller. Dawn of the transformer era in speech emotion recognition: closing the valence gap. *IEEE Transactions on Pattern Analysis and Machine Intelligence*, 45(9):10745–10759, 2023.
- [13] Xin Li, Yu Tong, and Wen Wang. Medc: a literature analysis system for chinese medicine research. In *Smart Health: International Conference, ICSH 2015, Phoenix, AZ, USA, November 17-18, 2015. Revised Selected Papers*, pages 311–320. Springer, 2016.
- [14] Philip Jackson and SJUoSG Haq. Surrey audio-visual expressed emotion (savee) database. *University of Surrey: Guildford, UK*, 2014.
- [15] Steven R Livingstone and Frank A Russo. The ryerson audio-visual database of emotional speech and song (ravdess): A dynamic, multimodal set of facial and vocal expressions in north american english. *PloS one*, 13(5):e0196391, 2018.
- [16] Houwei Cao, David G Cooper, Michael K Keutmann, Ruben C Gur, Ani Nenkova, and Ragini Verma. Crema-d: Crowd-sourced emotional multimodal actors dataset. *IEEE transactions on affective computing*, 5(4):377–390, 2014.
- [17] Kate Dupuis and M Kathleen Pichora-Fuller. Recognition of emotional speech for younger and older talkers: Behavioural findings from the toronto emotional speech set. *Canadian Acoustics*, 39(3):182–183, 2011.
- [18] Felix Burkhardt, Astrid Paeschke, Miriam Kienast, Walter F. Sendlmeier, and Benjamin Weiss. Berlin emodb, December 2022.
- [19] Giovanni Costantini, Iacopo Iaderola, Andrea Paoloni, and Massimiliano Todisco. EMOVO corpus: an Italian emotional speech database. In Nicoletta Calzolari, Khalid Choukri, Thierry Declerck, Hrafn Loftsson, Bente Maegaard, Joseph Mariani, Asuncion Moreno, Jan Odijk, and Stelios Piperidis, editors, *Proceedings of the Ninth International Conference on Language Resources and Evaluation (LREC'14)*, pages 3501–3504, Reykjavik, Iceland, May 2014. European Language Resources Association (ELRA).
- [20] Haoran Sun, Dong Wang, Lantian Li, Chen Chen, and Thomas F Zheng. Random cycle loss and its application to voice conversion. *IEEE Transactions on Pattern Analysis and Machine Intelligence*, 45(8):10331–10345, 2023.
- [21] Corinna Cortes and Vladimir Vapnik. Support-vector networks. *Machine learning*, 20:273–297, 1995.
- [22] Sugaan Nagarajan, Satya Sai Srinivas Nettimi, Lakshmi Sutha Kumar, Malaya Kumar Nath, and Aniruddha Kanhe. Speech emotion recognition using cepstral features extracted with novel triangular filter banks based on bark and erb frequency scales. *Digital Signal Processing*, 104:102763, 2020.
- [23] M Othman, A Wahab, and R Khosrowabadi. Mfcc for robust emotion detection using eeg. In *2009 IEEE 9th Malaysia international conference on communications (MICC)*, pages 98–101. IEEE, 2009.
- [24] Samson Akinpelu, Serestina Viriri, and Adekanmi Adegun. An enhanced speech emotion recognition using vision transformer. *Scientific Reports*, 14(1):13126, 2024.
- [25] Alexey Dosovitskiy, Lucas Beyer, Alexander Kolesnikov, Dirk Weissenborn, Xiaohua Zhai, Thomas Unterthiner, Mostafa Dehghani, Matthias Minderer, Georg Heigold, Sylvain Gelly, et al. An image is worth 16x16 words: Transformers for image recognition at scale. *arXiv preprint arXiv:2010.11929*, 2020.
- [26] Ciaran Cooney, Rafaella Folli, and Damien Coyle. Mel frequency cepstral coefficients enhance imagined speech decoding accuracy from eeg. In *2018 29th Irish Signals and Systems Conference (ISSC)*, pages 1–7, 2018.
- [27] T Mary Little Flower and T Jaya. Speech emotion recognition using ramanujan fourier transform. *Applied Acoustics*, 201:109133, 2022.
- [28] Pengxu Jiang, Hongliang Fu, Huawei Tao, Peizhi Lei, and Li Zhao. Parallelized convolutional recurrent neural network with spectral features for speech emotion recognition. *IEEE access*, 7:90368–90377, 2019.



- [29] Turker Tuncer, Sengul Dogan, and U Rajendra Acharya. Automated accurate speech emotion recognition system using twine shuffle pattern and iterative neighborhood component analysis techniques. *Knowledge-Based Systems*, 211:106547, 2021.
- [30] J Ancilin and A Milton. Improved speech emotion recognition with mel frequency magnitude coefficient. *Applied Acoustics*, 179:108046, 2021.
- [31] Muddasar Laghari, Muhammad Junaid Tahir, Abdullah Azeem, Waqar Riaz, and Yi Zhou. Robust speech emotion recognition for sindhi language based on deep convolutional neural network. In *2021 international conference on communications, information system and computer engineering (CISCE)*, pages 543–548. IEEE, 2021.
- [32] Changjiang Jiang, Junliang Liu, Rong Mao, and Sifan Sun. Speech emotion recognition based on dcnn bigru self-attention model. In *2020 International Conference on Information Science, Parallel and Distributed Systems (ISPDS)*, pages 46–51. IEEE, 2020.
- [33] JTFLM Zhang and Huibin Jia. Design of speech corpus for mandarin text to speech. In *The blizzard challenge 2008 workshop*, 2008.
- [34] Mingxu Feng, Tianshu Fang, Chaozhu He, Mengqian Li, and Jizhong Liu. Affect and stress detection based on feature fusion of lstm and ldcnn. *Computer Methods in Biomechanics and Biomedical Engineering*, 27(4):512–520, 2024.
- [35] Jie Xie, Mingying Zhu, and Kai Hu. Fusion-based speech emotion classification using two-stage feature selection. *Speech Communication*, 152:102955, 2023.
- [36] Hua Wang, Wenchuan Wang, Yujin Du, and Dongmei Xu. Examining the applicability of wavelet packet decomposition on different forecasting models in annual rainfall prediction. *Water*, 13(15):1997, 2021.
- [37] Mustaqeem and Kwon Soonil. A cnn-assisted enhanced audio signal processing for speech emotion recognition. *Sensors*, 20(1):183, 2019.
- [38] Ismail Shahin, Noor Hindawi, Ali Bou Nassif, Adi Alhudhaif, and Kemal Polat. Novel dual-channel long short-term memory compressed capsule networks for emotion recognition. *Expert Systems with Applications*, 188:116080, 2022.
- [39] Povilas Treigys, Gražina Korvel, Gintautas Tamulevičius, Jolita Bernatavičienė, and Božena Kostek. Investigating feature spaces for isolated word recognition. *Data science: New issues, challenges and applications*, pages 165–181, 2020.
- [40] Jacob Devlin, Ming-Wei Chang, Kenton Lee, and Kristina Toutanova. Bert: Pre-training of deep bidirectional transformers for language understanding. In *Proceedings of the 2019 conference of the North American chapter of the association for computational linguistics: human language technologies, volume 1 (long and short papers)*, pages 4171–4186, 2019.
- [41] Yinhan Liu, Myle Ott, Naman Goyal, Jingfei Du, Mandar Joshi, Danqi Chen, Omer Levy, Mike Lewis, Luke Zettlemoyer, and Veselin Stoyanov. Roberta: A robustly optimized bert pretraining approach. *arXiv preprint arXiv:1907.11692*, 2019.
- [42] Mani Kumar Tellamekala, Shahin Amiriparian, Björn W Schuller, Elisabeth André, Timo Giesbrecht, and Michel Valstar. Cold fusion: Calibrated and ordinal latent distribution fusion for uncertainty-aware multimodal emotion recognition. *IEEE Transactions on Pattern Analysis and Machine Intelligence*, 46(2):805–822, 2023.
- [43] Rahul Dey and Fathi M Salem. Gate-variants of gated recurrent unit (gru) neural networks. In *2017 IEEE 60th international midwest symposium on circuits and systems (MWSCAS)*, pages 1597–1600. IEEE, 2017.
- [44] Zheng Lian, Lan Chen, Licai Sun, Bin Liu, and Jianhua Tao. Gcnet: Graph completion network for incomplete multimodal learning in conversation. *IEEE Transactions on pattern analysis and machine intelligence*, 45(7):8419–8432, 2023.
- [45] Jingting Li, Zizhao Dong, Shaoyuan Lu, Su-Jing Wang, Wen-Jing Yan, Yinhuan Ma, Ye Liu, Changbing Huang, and Xiaolan Fu. Cas (me) 3: A third generation facial spontaneous micro-expression database with depth information and high ecological validity. *IEEE Transactions on Pattern Analysis and Machine Intelligence*, 45(3):2782–2800, 2022.
- [46] Changchong Sheng, Gangyao Kuang, Liang Bai, Chenping Hou, Yulan Guo, Xin Xu, Matti Pietikäinen, and Li Liu. Deep learning for visual speech analysis: A survey. *IEEE Transactions on Pattern Analysis and Machine Intelligence*, 2024.
- [47] Carlos Busso, Murtaza Bulut, Chi-Chun Lee, Abe Kazemzadeh, Emily Mower, Samuel Kim, Jeannette N Chang, Sungbok Lee, and Shrikanth S Narayanan. Iemocap: Interactive emotional dyadic motion capture database. *Language resources and evaluation*, 42:335–359, 2008.

- [48] Soujanya Poria, Devamanyu Hazarika, Navonil Majumder, Gautam Naik, Erik Cambria, and Rada Mihalcea. Meld: A multimodal multi-party dataset for emotion recognition in conversations. *arXiv preprint arXiv:1810.02508*, 2018.
- [49] Xiangyu Wang and Chengqing Zong. Learning emotion category representation to detect emotion relations across languages. *IEEE Transactions on Pattern Analysis and Machine Intelligence*, 2025.
- [50] M. Kathleen Pichora-Fuller and Kate Dupuis. Toronto emotional speech set (TESS), 2020.
- [51] Sanaul Haq, Philip JB Jackson, and James D Edge. Audio-visual feature selection and reduction for emotion classification. In *AVSP*, pages 185–190, 2008.
- [52] Paul Heckbert. Fourier transforms and the fast fourier transform (fft) algorithm. *Computer Graphics*, 2(1995):15–463, 1995.
- [53] Nasir Ahmed, T\_ Natarajan, and Kamisetty R Rao. Discrete cosine transform. *IEEE transactions on Computers*, 100(1):90–93, 2006.
- [54] Anqi Mao, Mehryar Mohri, and Yutao Zhong. Cross-entropy loss functions: Theoretical analysis and applications. In *International conference on Machine learning*, pages 23803–23828. PMLR, 2023.
- [55] Mohamed Reyad, Amany M Sarhan, and Mohammad Arafa. A modified adam algorithm for deep neural network optimization. *Neural Computing and Applications*, 35(23):17095–17112, 2023.
- [56] T Mary Little Flower and T Jaya. A novel concatenated 1d-cnn model for speech emotion recognition. *Biomedical Signal Processing and Control*, 93:106201, 2024.
- [57] Muhammad Sajjad, Soonil Kwon, et al. Clustering-based speech emotion recognition by incorporating learned features and deep bilstm. *IEEE access*, 8:79861–79875, 2020.
- [58] Nicolae-Catalin Ristea and Radu Tudor Ionescu. Self-paced ensemble learning for speech and audio classification. *arXiv preprint arXiv:2103.11988*, 2021.
- [59] Zeynep Hilal Kilimci, Ulku Bayraktar, and Ayhan Kucukmanisa. Evaluating raw waveforms with deep learning frameworks for speech emotion recognition. *arXiv preprint arXiv:2307.02820*, 2023.
- [60] Sakorn Mekruksavanich, Anuchit Jitpattanakul, and Narit Hnoohom. Negative emotion recognition using deep learning for thai language. In *2020 joint international conference on digital arts, media and technology with ECTI northern section conference on electrical, electronics, computer and telecommunications engineering (ECTI DAMT & NCON)*, pages 71–74. IEEE, 2020.
- [61] Hira Dhamyal, Benjamin Elizalde, Soham Deshmukh, Huaming Wang, Bhiksha Raj, and Rita Singh. Describing emotions with acoustic property prompts for speech emotion recognition. *arXiv preprint arXiv:2211.07737*, 2022.
- [62] Lucas Goncalves, Seong-Gyun Leem, Wei-Cheng Lin, Berrak Sisman, and Carlos Busso. Versatile audio-visual learning for handling single and multi modalities in emotion regression and classification tasks. *arXiv preprint arXiv:2305.07216*, 2023.
- [63] Palani Thanaraj Krishnan, Alex Noel Joseph Raj, and Vijayarajan Rajangam. Emotion classification from speech signal based on empirical mode decomposition and non-linear features: Speech emotion recognition. *Complex & Intelligent Systems*, 7:1919–1934, 2021.
- [64] Hao Meng, Tianhao Yan, Fei Yuan, and Hongwei Wei. Speech emotion recognition from 3d log-mel spectrograms with deep learning network. *IEEE access*, 7:125868–125881, 2019.
- [65] Zheng Liu, Xin Kang, and Fuji Ren. Dual-tbnet: Improving the robustness of speech features via dual-transformer-bilstm for speech emotion recognition. *IEEE/ACM Transactions on Audio, Speech, and Language Processing*, 31:2193–2203, 2023.
- [66] Aditya Dutt and Paul Gader. Wavelet multiresolution analysis based speech emotion recognition system using 1d cnn lstm networks. *IEEE/ACM Transactions on Audio, Speech, and Language Processing*, 31:2043–2054, 2023.